High Field Side Lower Hybrid Current Drive Simulations for Off-axis Current Drive in DIII-D

S.J. Wukitch[1,*], *S.* Shiraiwa[1], *G.M.* Wallace[1], *P.T.* Bonoli[1], *C.* Holcomb[2], and *R.I.* Pinsker[3]

[1]Massachusetts Institute of Technology, Plasma Science and Fusion Center, Cambridge, Massachusetts 02139, USA
[2]Lawrence Livermore National Laboratory, Livermore, California 94551, USA
[3]General Atomics, P.O. Box 85608, San Diego, California 92186-5608, USA

Abstract. Efficient off-axis current drive scalable to reactors is a key enabling technology for developing economical, steady state tokamak. Previous studies have focussed on high field side (HFS) launch of lower hybrid current drive (LHCD) in double null configurations in reactor grade plasmas and found improved wave penetration and high current drive efficiency with driven current profile peaked near a normalized radius, ρ, of 0.6-0.8, consistent with advanced tokamak scenarios. Further, HFS launch potentially mitigates plasma material interaction and coupling issues. For this work, we sought credible HFS LHCD scenario for DIII-D advanced tokamak discharges through utilizing advanced ray tracing and Fokker Planck simulation tools (GENRAY+CQL3D) constrained by experimental considerations. For a model and existing discharge, HFS LHCD scenarios with excellent wave penetration and current drive were identified. The LHCD is peaked off axis, ρ~0.6-0.8, with FWHM $\Delta\rho$=0.2 and driven current up to 0.37 MA/MW coupled. For HFS near mid plane launch, wave penetration is excellent and have access to single pass absorption scenarios for variety of plasmas for $n_\parallel$=2.6-3.4. These DIII-D discharge simulations indicate that HFS LHCD has potential to demonstrate efficient off axis current drive and current profile control in DIII-D existing and model discharge.

Introduction

Efficient off-axis current drive (OACD) scalable to reactors is a key enabling technology for economical, steady state tokamak. Efficient OACD scalable to reactors is yet to be demonstrated both from efficiency and survivability perspective. Studies of reactor grade, double null plasmas utilizing high field side (HFS) launch lower hybrid current drive (LHCD) have found improved wave penetration enabling efficient OACD.[1] Further, HFS launch potentially mitigates plasma material interaction and coupling issues due to quiescent HFS scrape off layer (SOL)[2], lower plasma particle[3] and neutron flux, and improved impurity screening[4]. HFS LHCD in DIII-D discharges offer an opportunity to validate HFS wave physics and SOL benefits for RF actuators.

In addition to primarily RF constraints, the analysis presented here optimizes for scenarios compatible with DIII-D advanced tokamak and scenario development research.[5] A key ingredient is current profile optimization.[6] Given the existing and planned DIII-D off axis current drive actuators (neutral beam[7], electron cyclotron[8], and helicon[9]), the HFS LHCD is to drive current at normalized minor radius, ρ, in the range of 0.6-0.8 with current density approaching 0.4 MA/m^2 for fields down to 1.6 T with central densities approaching 1×10^{20} m^{-3}. The goal of this work is to identify a credible HFS LHCD scenario for DIII-D. The simulation tool utilized in this study is GENRAY+CQL3D (advanced ray tracing and Fokker Planck solver[10,11]) for which existing and model DIII-D discharges were investigated.

The motivation to investigate HFS LHCD in DIII-D derives from the possibility to significantly improve the wave penetration and absorption compared to low field side (LFS) launch. For lower hybrid (LH) waves, wave access is a set by wave accessibility[12]and the condition for electron Landau damping[13]. For a given wave frequency, the minimum index of refraction, $n_\parallel$, that will penetrate into plasma is proportional to $n_e^{1/2}/B$ where n_e is plasma density and B is magnetic field. Ideally, the wave penetrates into the plasma until electron Landau damped which can be expressed as $n_\parallel \geq (30/T_e)^{1/2}$ where T_e is electron temperature in keV[14]. On the HFS, the toroidal field is higher and allows launch of lower $n_\parallel$ waves that penetrate farther into the plasma core before damping. A further benefit to lower $n_\parallel$ launch is that the waves are absorbed at higher T_e yielding a higher current drive efficiency, ~$1/n_\parallel^2$, because wave momentum is transferred to less collisional electrons.[15] Looking towards reactor concepts where current drive efficiency is the primary parameter to be optimized, the poloidal position is selected to balance the effects of toroidicity

---
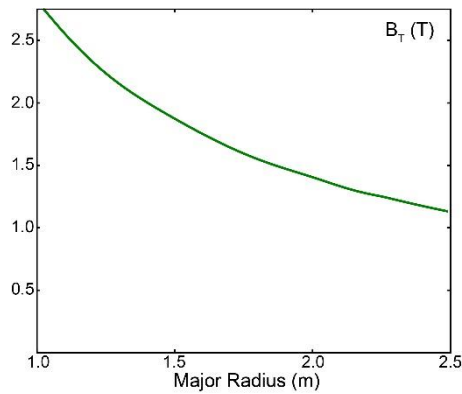
Fig. 1 Magnetic field profile for 147634 (1.66 T discharge) shows that the HFS local magnetic field is 2.5x the LFS value.
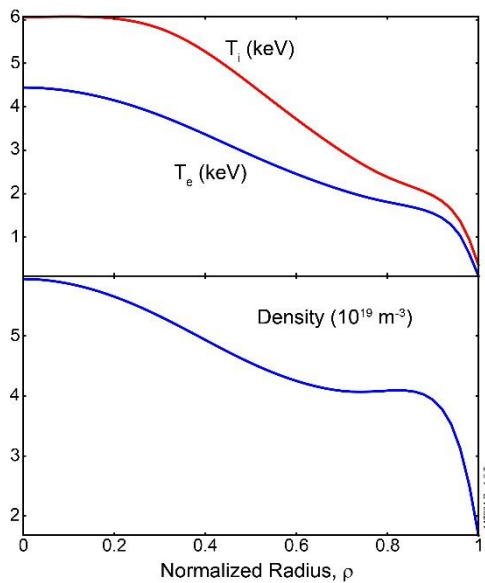
**Fig. 2** Electron density, ion and electron temperature profiles are peaked.

and poloidal field to maintain the smallest $n_\parallel$ possible. In DIII-D, the primary consideration is the damping location. Thus, proper poloidal positioning allows for waves to penetrate and damp in region $\rho\sim0.6$-0.8.

HFS LHCD Scenario Identification

As mentioned above, LFS LHCD is unattractive in DIII-D and reactor plasmas due to wave penetration into the plasma core.[1] Using a typical low q_{min} (q is safety factor) discharge (147634), the mid plane B-field, density electron and ion temperature profiles are shown in figure 1 and 2. The waves launched with $n_\parallel$=2.7 at 4.6 GHz from the outboard mid plane fail to penetrate into the plasma core and pass through the divertor region as shown in figure 3. The discharge profiles are representative of profiles in other DIII-D advanced tokamak (AT) and model discharges investigated here. The study examined a variety of discharges with different launcher locations to identify launch positions to optimize wave penetration, absorption location, and current drive efficiency. The waves were launched assuming four poloidal locations to represent an
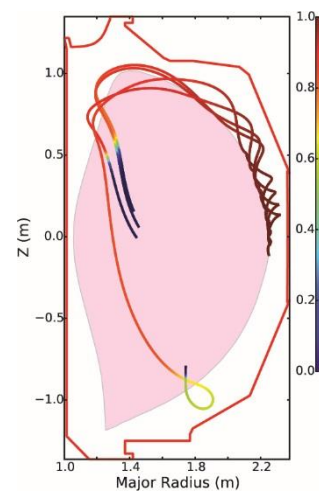
Fig. 3 LH waves launched from LFS mid plane remain in the plasma periphery for 147634 due to the density and low local B field.
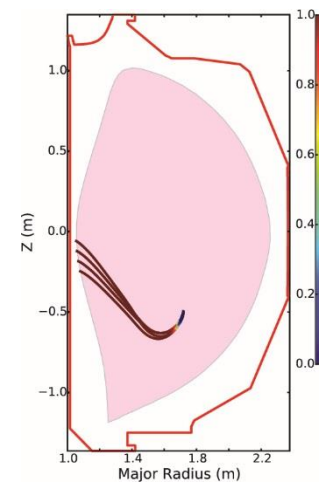
**Fig. 4** LH waves launched from HFS near mid plane penetrate and single pass damp near $\rho\sim0.6$ for 147634.

expected coupler with a spectrum peaked near 2.7 and width of +/-0.2 which is consistent with 32 toroidal apertures. Two HFS launch positions showed the greatest promise: near the upper divertor and near the mid plane.

An example of near mid plane HFS launch position is shown in figure 4. The rays are launched at poloidal positions 3-24 cm below the mid plane. The launch spectrum has a peak at $n_\parallel$=2.7+/-0.2. The rays penetrate and drive ~150 kA/MW peaked near $\rho\sim0.6$ with a corresponding efficiency 0.12×10^{20} A*W^{-1}m^{-2}. As shown in Figure 5, the simulation suggests with 1 MW of coupled power can satisfy the required OACD in the range of $\rho\sim0.6$-0.8 with current density approaching 0.4 MA/m^2 for AT discharges. The ray penetration and trajectory are sensitive to $n_\parallel$ and poloidal launch position. The rays from -3 cm propagate to the largest Z values with a few rays, $n_\parallel\sim2.5$, refracting back to the plasma edge at the top of the device. Launching the rays at or above the mid plane results in many more rays becoming trapped in the plasma edge.
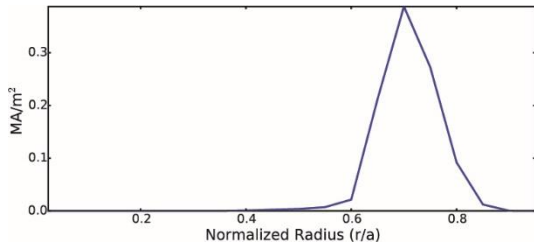
An example of near upper divertor HFS launch position is shown in figure 6. The rays are launched at poloidal
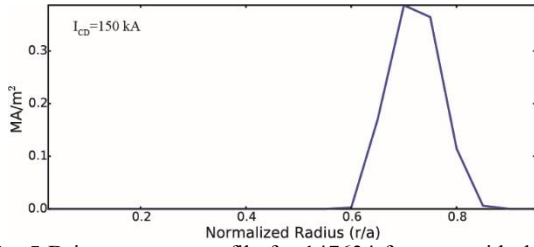
Fig. 5 Driven current profile for 147634 for near mid plane launch is peaked near ρ~0.6 and approaching the required 0.4 MA/m^2 with 1 MW coupled.
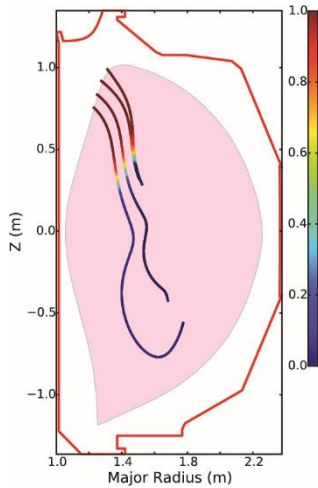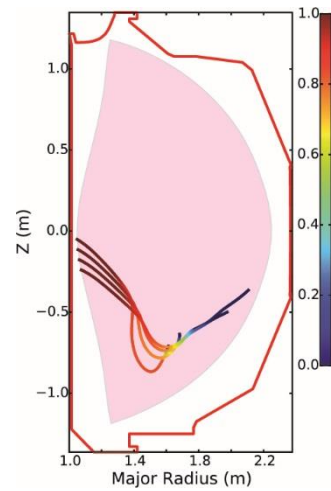

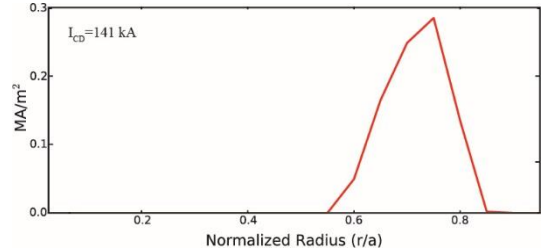**Fig. 6** Ray propagation for near upper divertor LH wave launch shows good wave penetration and absorption.

Fig. 7 Driven current profile is peaked near ρ~0.7 with ~140 kA driven current.

Fig. 8 For DIII-D model AT discharge (1.6 T), HFS launched near mid plane penetrate and has single pass damping.

Fig. 9 Driven current profile for 1.6 T, DIII-D model AT discharge is peaked near ρ~0.7 for near mid plane launch.
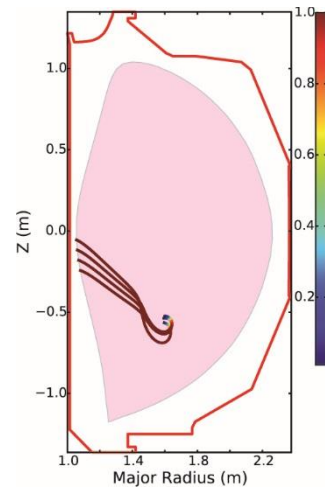
Fig. 10 For 144476 (2 T), HFS launch has excellent wave penetration and single pass damp near r~0.6.
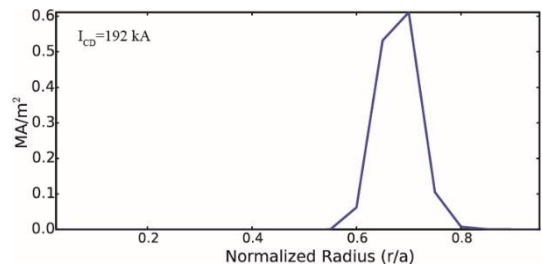
Fig. 11 Driven current profile for 144476 (2 T) DIII-D AT discharge for n∥=2.6+/-0.2 is peaked near r~0.7 and drives ~190 kA/MW with current density >0.4 MA/m^2.

positions 0.85 to 1.0 m above the mid plane. The launch spectrum is peaked at n∥=2.7+/-0.2. The rays penetrate and damp near ρ~0.7 and drive ~140 kA per MW coupled peaked with a corresponding efficiency 0.1×10^{20} A*W^{-1}m^{-2} as shown in Fig. *7*. Moving the launch location to closer to the mid plane results in decreased penetration and multiple reflections. Although similar to the near mid plane launch in penetration and efficiency, the near upper divertor launch has practical considerations that make it less ideal. For upper discharges with upper X-points, the launcher would be in a zone of high heat flux and high density. The former would make a structure difficult to design and the latter may prevent the waves from penetrating into the plasma. Further, long distance coupling would be very challenging. The anticipated long distance coupling, the distance to the last closed flux surface (LCFS), is >10 cm.
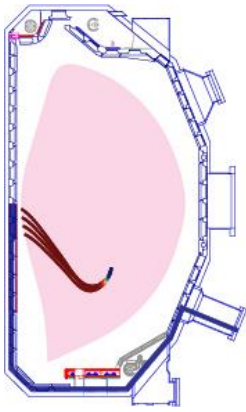
For near mid plane launch, the sensitivity to magnetic field, electron temperature, and density were examined. The general trend with B-field is n∥ required for damping at ρ~0.6-0.8 increased to 3 as B-field decreased to 1.6 T.

Fig 8 and 9 show the wave propagation and driven current for a DIII-D 1.6 T AT discharge. For n∥=3+/-0.2,

Fig. 12 The wave guide route fits within the in-vessel profile except on the inner wall and baffle plate.
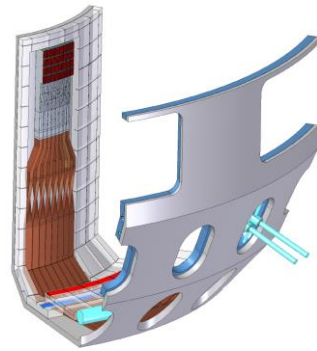
Fig. 13 Placement of HFS LHCD coupler and wave guide network in the DIII-D model vacuum vessel is challenging but appears plausible assuming one can increase the radius of the center column tiles 2.5 cm.

the waves propagate and drive ~150 kA/MW current between ρ~0.6-0.8. To obtain 0.4 MA/m^2 for this discharge, the HFS LHCD power would need to couple ~1.3 MW. At ~2 T, the higher field allows a lower $n_\parallel$ to be launched and the corresponding driven current increases to 190 kA/MW. At this level, the current density is sufficient to allow current profile control from a simulation perspective. Similar studies were done for density and temperature. As expected increasing the density required increasing $n_\parallel$ to 3.4 for central density ~9×10^{20} m^{-3} at 1.6 T and the driven current falls to ~85 kA/MW. At higher B-fields, the density window and driven current levels improve. For temperature, the primary impact was on single pass damping. Decreasing the temperature by 25% from existing discharges resulted in waves having multiple reflections where ~85% of the power is damped on the first pass.

Practical Outlook for HFS LHCD at DIII-D

The conceptual launcher and wave guide network design is based on existing technology and is shown in Fig 12 and Fig 13. One WR-187 wave guide from a 250 kW klystron will be split into 16 apertures using two bi-junctions[16] toroidally and a 4 way poloidal splitter[17]. The conceptual launcher is eight WR-187 split into 32 toroidal apertures. This results in an expected power density of <30 MW/m^2 assuming 200 kW delivered and similar to power densities obtained in Tore Supra and planned for ITER.[16] The aperture dimension is 6 cm tall and 0.5 cm wide with a 1 mm septa and results in a peak $n_\parallel$=2.7 for $\Delta\phi$=90° excitation. With the passive elements, the directivity is ~62% and can access 2.4≤$n_\parallel$≤3 with >55% directivity. The wave guide enters from the LFS, passes under the cryopump and divertor and up the inner wall with the long dimension along the vessel. Above the inner strike point, the wave guide twists to orient the wave guide's long dimension perpendicular to the inner column. To accommodate the twist, the inner column radius would need to increase by 2.54 cm. For the AT plasmas simulated here, the smallest inner gap is 3.8 cm suggesting there is may be room to expand the inner column without impacting the target AT plasmas. In addition to the inner column tile modifications, a number of protective tiles and baffle plate would need to be modified to allow routing of the wave guides to the launcher. From an operational perspective, impurities from a metal surface on the inner wall needs to be assessed.

Summary of HFS LHCD at DIII-D

The simulations suggest efficient HFS LHCD off-axis current drive is possible for DIII-D existing and target AT discharges. An experiment based on these simulations could provide an opportunity to demonstrate q profile control for B_T≥1.6 T, n_e<9×10^{19}m^{-3} with high current drive efficiency and deposition peaked between ρ=0.6-0.8 compatible with high temperature plasmas and scalable to reactors. Further, such an experiment would allow investigation of HFS wave propagation and SOL benefits for RF actuators. The primary in-vessel challenge is increase of the central column radius.

References

[1] P.T. Bonoli et al., "Novel Reactor Relevant RF Actuator Schemes for the Lower Hybrid and the Ion Cyclotron Range of Frequencies". Preprint: 2016 IAEA Fusion Energy Conference, Kyoto [TH/5-1].

[2] N. Smick, B. Labombard, and I.H. Hutchinson, Nuclear Fusion **53**, 023001 (2013).

[3] B. LaBombard, J.E. Rice, A.E. Hubbard, J.W. Hughes et al., Nuclear Fusion **44**, 1047 (2004).

[4] B. Labombard, A. Kuang, D. Brunner, I. Faust et al., Nuclear Fusion **57**, -76021 (2017).

[5] T. C. Luce, Fusion Sci. Tech. **48**, 1212–1225 (2005).

[6] C. T. Holcomb, J. R. Ferron, T. C. Luce, T. W. Petrie, et al. Nuclear Fusion **54**, 093009 (2014).

[7] J. M. Park, M. Murakami, C. C. Petty, W. W. Heidbrink et al., Phys. Plasmas **16**, 092508 (2009).

[8] R. Prater and C. C. Petty, Fusion Sci. Tech. **48**, 1141–1148 (2005).

[9] R. Prater, C. P. Moeller, R. I. Pinsker, M. Porkolab et al., Nucl. Fusion **54**, 083024 (2014).

[10] A.P. Smirnov and R.W. Harvey, Bull. Am. Physical Society **40**, 1837 (1995).

[11] R. W. Harvey, and M. McCoy, in Proceedings of the IAEA Technical Committee Meeting on Simulation and Modeling of Thermonuclear Plasmas, Montreal, Canada, 1992 (IAEA, Vienna, 1992), US DOC NTIS Document No. DE93002962.

[12] M. Brambilla Nuc. Fusion **19**, 1357 (1979).

[13] M. Brambilla Physics of Plasma Close to Thermonuclear Conditions (Brussels, 1980) 291.

[14] Y. Peysson and Tore Supra Team, Nuclear Fusion **41**, 1703 (2001). doi:10.1088/0029-5515/41/11/320.

[15] N. J. Fisch, Phys. Rev. Lett. **41**, 873 (1978).

[16] A. Bécoulet, Ph. Bibet, F. Mirizzi, M.L. Apicella et al., Fus. Eng. Design **86**, 490–496 (2011).

[17] S. Shiraiwa O. Meneghini, R.R. Parker, G. Wallace et al., Nucl. Fusion **51**, 103024 (2011).